Indian Geotech J
https://doi.org/10.1007/s40098-025-01222-6

ORIGINAL PAPER

Integration of Landslide Susceptibility and Road Infrastructure Vulnerability for Risk Assessment and Mountain Road Resilience Enhancement

Keshab Kumar Sharma[1] · **Netra Prakash Bhandary**[2] · **Mandip Subedi**[3,4] · **K. C. Rajan**[4]

Received: 9 January 2025 / Accepted: 14 March 2025

Abstract Roadways are the most common mode of transport because they offer last-mile connectivity and are user friendly. In hilly and mountainous regions, however, most roads are vulnerable to landslides, posing significant disruption in traffic movement as well as risk to human life and property. Understanding these road vulnerabilities is important for ensuring the smooth operation and safety of transportation service. This paper aims to explore the risk of landslides to road and road infrastructure along the Narayanghat–Kathmandu road section in Nepal, and for this, we have taken into account 11 landslide conditioning factors and created a landslide susceptibility map of the study area, employing the analytical hierarchy process (AHP) in the geographic information system (GIS) platform. The performance of the susceptibility model was evaluated by area under the receiver operating characteristic (ROC) technique using 122 historical landslide inventory datasets. Subsequently, considering seven critical road infrastructure elements at risk, landslide vulnerability map was prepared for the target roadway. By combining susceptibility and vulnerability maps, a disaster risk map was generated. From the obtained results, it was understood that several key components of the road infrastructure in the study area are located at high-risk zone, which include four bridges, thirty two culverts, thirty two retaining walls, twelve safety blocks, and two delineators. The significance of this study is at mitigating the adverse impacts of landslides on roadway infrastructure and improving the safety and reliability of transportation network in mountainous regions.

Keywords Landslide susceptibility · Analytical hierarchy process · Road infrastructure vulnerability · Risk assessment

Introduction

Road networks play a crucial role in supporting economic activities and fostering social connectivity for the development of a nation [27]. However, particularly on hilly and mountainous terrains, roads are prone to frequent damage due to slope failures and landslides, which are one of the most common natural hazards in mountainous areas and pose significant threat to highway safety and integrity [17, 37, 42]. Landslides result from a complex interplay of several factors including geology, geomorphology, and subsurface hydrology exacerbated by triggering factors like earthquake, rainfall, erosion, land use pattern and so on [32, 47]. Moreover, anthropogenic activities, such as construction of hill roads disturb the natural slope stability and increase the chances of landsliding [3, 38], which not only disrupts the road traffic but also endanger human life in the vicinity and hinder socio-economic activities [23, 28]. So, a comprehensive landslide risk assessment along the roads of high socio-economic importance can be considered essential for effective road infrastructure planning and transport management, especially in developing nations where roadside slope management and neighborhood landslide prevention system are still at minimum level [13].

✉ Netra Prakash Bhandary
netra@ehime-u.ac.jp

[1] Ministry of Physical Infrastructure and Transport, Government of Nepal, Kathmandu, Nepal

[2] Graduate School of Science and Engineering, Ehime University, Matsuyama, Japan

[3] Universal Engineering and Science College, Lalitpur, Nepal

[4] Geoinfra Research Institute, Lalitpur, Nepal

Published online: 09 April 2025

Landslide risk assessment involves a comprehensive analysis of both susceptibility and vulnerability factors for accurately evaluating the potential impact of landslides [6, 20]. Landslide susceptibility refers to the likelihood of landslide occurrence based on terrain conditions such as slope, geology, and rainfall, while vulnerability represents the degree of potential damage to road infrastructure and other elements exposed to landslides [5, 8]. Integrating both susceptibility and vulnerability, we consider that landslide risk assessment could be made more comprehensive. In recent years, spatial assessment of susceptibility and vulnerability have emerged as a suitable approach to evaluating the landslide risk, especially due to advancement in analytical tools, technology, and accessibility to spatial and multi-temporal data. By integrating geospatial data layers and employing advanced analytical techniques, such as landslide susceptibility mapping and vulnerability assessment, risky areas can be accurately identified.

While dealing with the mountain road issues, most previous studies focus more on landslide susceptibility evaluation, but they do not consider road infrastructure vulnerability or concentrate more on the road network vulnerability while overlooking the landslide hazard. For example, Panchal and Shrivastava [23] use AHP model to produce a landslide hazard map for an Indian National Highway integrating 10 causative factors and assigning weights to these factors. Likewise, Sur et al. [41] develop a susceptibility map for the Kalsi–Chakrata Road corridor in India using 14 landslide conditioning factors and employing fuzzy AHP technique. Alsabhan et al. [4] also prepare a landslide susceptibility map along the Kasauli–Parwanoo road corridor and divide the area into five susceptibility zones. Slightly different from these studies, however, Zou et al. [50] develop an integrated model for the highway vulnerability assessment. They consider environmental sensibility, structural properties, and functional impact of the highway infrastructure as well as exposure probability and quantity of mobile hazard-affected objects. Likewise, Lu et al. [19] develop an approach to assess road network vulnerability examining the road alignment and various types of degradation under accidents. They validate this approach on Florida highway network. To overcome this constraint of focusing solely on either landslide susceptibility or road infrastructure vulnerability, a multidimensional method of road network assessment combining landslide hazard factors with vulnerability of the disaster-prone entities is considered essential.

To address the aforementioned challenges and enhance the resilience of mountain roads, while circumventing the constraints of a singular approach, in this study, we integrate both landslide susceptibility and road infrastructure vulnerability using a weighted methodology to assess the landslide risk along one of the most important sections of the national road network in Nepal. We consider a total of 11 landslide conditioning factors for the landslide susceptibility analysis and take into account almost all existing road infrastructure elements for the vulnerability assessment. By integrating these two layers, we conduct a comprehensive evaluation of the landslide risk associated with the road infrastructure in the target area. We consider this integrated approach provides a robust foundation for informed decision-making and proactive planning of roadside slope safety measures. The insights from this research work may significantly contribute to enhancing the resilience of mountain roads. While the study primarily deals with the Narayanghat–Kathmandu roadway in Nepal, it holds universal applicability adaptable to diverse geographical contexts worldwide.

Study Area

We have conducted this study at one of the most important road routes in mid Nepal, which connects the capital city of Kathmandu with Narayanghat, a heavily populated city on the southern plains. The Narayanghat–Kathmandu road section in Nepal, a 146-km long bituminous double lane road, is also a part of the Asian Highway- 42 (AH42). This section of road network comprises of three national road sections: Narayanghat–Mugling section (36 km) of Narayanghat–Gorkha Highway, Mugling–Naubise section (84 km) of Prithvi Highway, and Naubise–Kathmandu section (26 km) of Tribhuvan Rajpath (Fig. 1). The annual average daily traffic (AADT) of this road section is 13,490 passenger car units (PCU) as of 2020–2021 data (MOPIT/DOR 2022). To fully capture the spatial distribution of risk factors, the landslide susceptibility study was carried out for the entire road stretch; however, the vulnerability assessment was limited to the Narayanghat–Mugling segment. This was done considering the ongoing upgradation work with reconstruction of pavement, drainage and support structures in Mugling–Kathmandu section which couldn't give the reliable results of structural vulnerability. Whereas the infrastructure in Narayanghat–Mugling segment is newly built (pavement and support structures 5 years ago and bridges completed last year). Therefore, Narayanghat–Mugling road segment was considered for the structural vulnerability assessment in this study.

As a mountainous country, Nepal suffers heavily from roadside landslides and slope failures, which make the road transportation system less efficient, such as by causing detours, delays, traffic jams, and increase the vehicle fuel consumption (as also stated by Ahmed [2]). Such road disruptions frequently occur during the rainy period (i.e., usually from June to August) and continue for a few days to a few weeks causing great inconvenience to road users. Timilsina and Dahal [43] mention that different mass movement types, such as debris flows, rockfalls, slope failures,

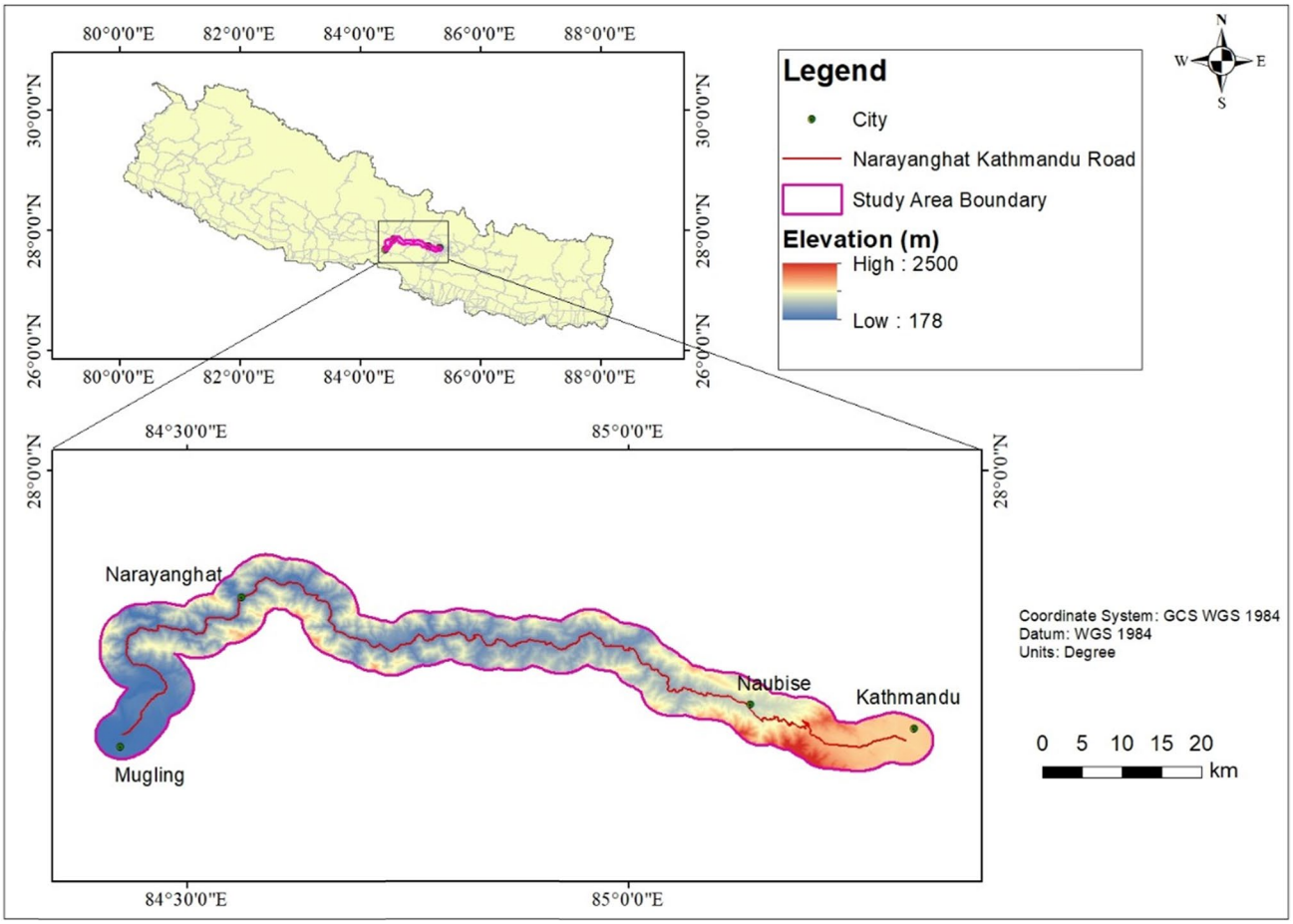

Fig. 1 Map showing the location of the study area, the Narayanghat–Kathmandu road section along with main reference points and elevation distribution

landslides are common in these road sections, especially along the Narayanghat–Mugling route. One major example of several days of road traffic disruption in the study area is due to frequently occurring landslides at Krishnabhir of Dhading district in 2001, which disrupted the traffic on Prithvi national roadway for 11 days [1]. In recent years too, the Narayanghat–Mugling section of the road was and still is frequently disrupted by landslides at several locations. The landslide and slope failure-related road traffic disruption situation is not less in other national roads too. These issues not only disrupt the traffic and affect the economy but also result in loss of human life and damage transport infrastructure, which incurs an annual direct economic loss of 11 million US dollars [11]. Moreover, these direct costs are much outweighed by the indirect losses from traffic closures and other socio-economic effects [7].

The southern part of the study area consists of plain terrain while the central north part consists of rolling hill slopes to steep slopes [31]. The elevation varies from 178 to 2500 m above mean sea level showcasing intricate topography, and the average annual precipitation in this region exceeds 1800 mm [24]. The target road section runs nearly parallel to one of the main river systems, the Trisuli River on its left bank while many tributaries from the left side of this river intersect the roadway.

Geologically, the Naubise–Kathmandu road section consists of two different rock masses of Precambrian age, namely the Bhimphedi formation consisting of medium grade metamorphic rock and Phulchauki formation consisting of relatively high-grade metamorphic rock [40]. The Mugling–Naubise road section crosses the midlands of the lesser Himalayan zone and consists of schist, phyllite, gneiss, quartzite, granite, and limestone as major rock types [7, 24]. Moreover, the Narayanghat–Mugling road section falls within Nuwakot Complex of the Lesser Himalayan zone on the north and Siwalik zones of central Nepal on the south [30]. The Nawakot Complex is composed of low-grade metamorphic rocks like slate, phyllite, quartzite and limestone, whereas the Siwalik Zone mainly consists of very soft loosely packed mudstones, siltstones, sandstones, shale, and conglomerates [7, 24, 31, 46]. The Narayanghat–Mugling road section intersects the Main Boundary Thrust (MBT),

a major tectonic thrust fault in the Himalayan region, and is also intercepted by several local faults.

Materials and Methods

An overall methodological framework adopted in the study is outlined in Fig. 2. This approach combines two crucial components; landslide susceptibility analysis and vulnerability assessment to evaluate the landslide risk in the study area. We used 11 key landslide conditioning factors; slope, elevation, slope aspect, profile curvature, land use land cover (LULC), normalized difference vegetation index (NDVI), geology, proximity to faults, distance from roads, distance to streams, and annual rainfall as the landslide conditioning factors, and adopted AHP (analytical hierarchy process) to generate the landslide susceptibility map. Because of their complementary nature, the NDVI and LULC were both included as landslide conditioning factors. While NDVI measures vegetation density and health, which affects slope stability, LULC offers a categorical classification of land types, aiding in the identification of human activities and land alterations. By collecting both detailed vegetation differences and broad land cover types, taking into account both elements increases the accuracy of landslide susceptibility mapping. The study area was delineated with a buffer of 300 m on the river side (right side) and 2000 m on the hill side (left side) of the roadway to encompass all potential influencing factors. The vulnerability assessment of the road transport infrastructure was done considering the roadside structures. By overlaying the roadside structure map with the landslide susceptibility map, we produced a comprehensive risk map, which facilitates the identification of landslide risk hotspots. The details of the materials and methods used in this study are presented in the following subsection.

Landslide Susceptibility Mapping

Data

Although landslide occurrence depends on the impact of various causal factors, in this work, we considered 11 landslide conditioning factors, as shown together with their sources of availability in Table 1. To validate the generated landslide susceptibility map, we assembled 74 historical landslide locations and prepared a landslide inventory map

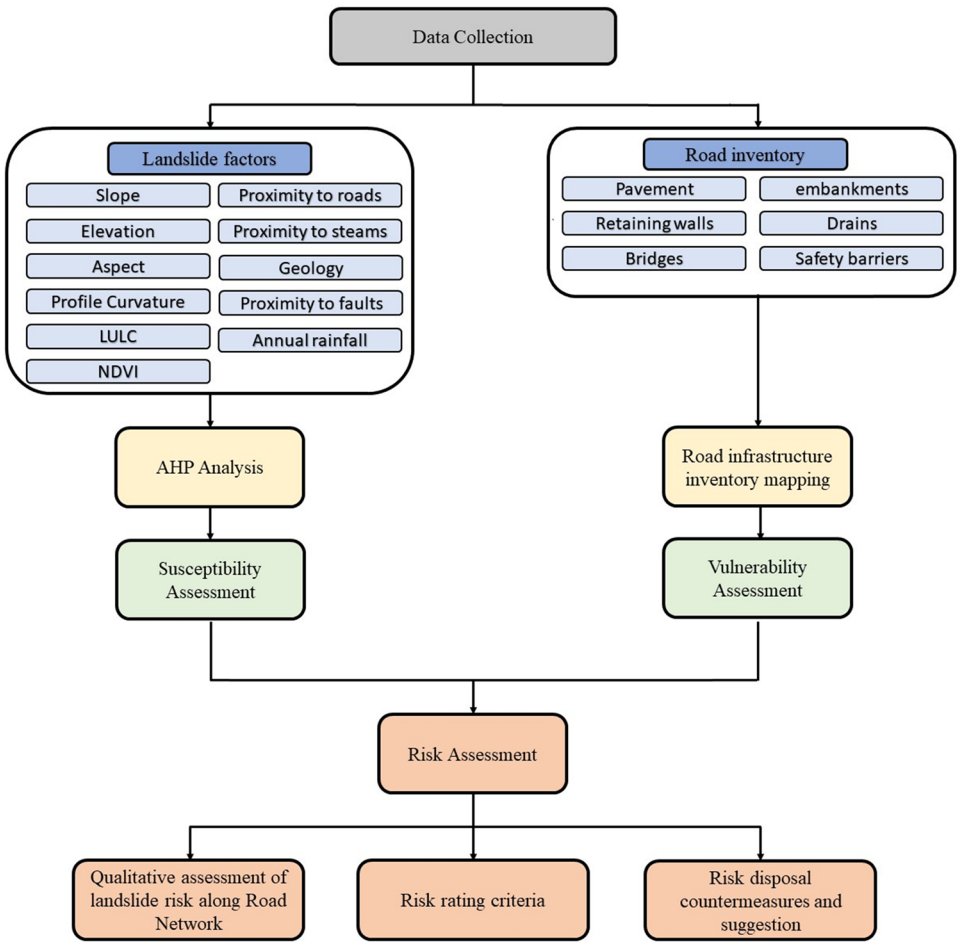

Fig. 2 Methodological flowchart for the landslide risk assessment

Table 1 Landslide conditioning factors used for the susceptibility analysis and their sources of availability

Variable	Source
Slope, elevation, aspect, curvature	ASTER Digital Elevation Model (DEM) (resolution: 30 m)
LULC, NDVI, proximity to road, proximity to streams	International Centre for Integrated Mountain Development (ICIMOD)
Geology	Department of Mines and Geology (DMG)
Proximity to faults	Literature review [31]
Annual rainfall	Climate Research Unit (CRU)

of the study area, which consists of 27 locations as obtained from the NASA Global rainfall-induced landslide catalog and 47 locations as mapped with the help of Google Earth images and verified through different sets of field visit. A few glimpses of the field visit observations are shown in Fig. 3. The landslide conditioning factors considered in this study are briefly described below.

Slope Slope is a key landslide conditioning factor, and it directly affects the stability of slopes by influencing the driving shear force. Steeper the slope, greater the likelihood of slope failure, but at the same time too steeper the slope, greater the likelihood of existence of intact rock slopes and lessen the chances of failure. Slope also influences the surface water flow and groundwater dynamics [49]. In this study, the slope map was prepared out of 30-m resolution DEM (digital elevation mode) data and was divided into five classes: (i) 0°–10°, (ii) 10°–20°, (iii) 20°–30°, (iv) 30°–40°, and v) above 40°. The assumption made for the slope class division is that 0°–10° (too gentle) and > 40° (too steep) slope classes have less number of landslides while 10°–40° slope classes have greater number of landslides.

Elevation Elevation is also a frequently used landslide conditioning factor while doing landslide susceptibility analysis [25]. In general, slopes at higher elevation are more prone to failure, as also stated by Yu et al. [48]. Zhou et al. [49] state that elevation determines the potential energy available for the movement. In this study, we prepared the elevation profile of the target area using the 30-m DEM data and divided it into five classes: (i) 180–300 m, (ii) 310–500 m, (iii) 510–700 m, (iv) 710–900 m, and (v) 910–1400 m for Narayanghat Mugling road section, (i) 236–400 (ii) 400–600 m (iii) 600–800 m (iv) 800–1000, and (v) 1000–1380 for Mugling–Naubise road section; and (i) 895–900 m (ii) 900–1200 m (iii) 1200–1500 m (iv) 1500–1800 m, and (v) 1800–2227 m for Naubise–Kathmandu road section.

Slope Aspect Slope aspect (i.e., the slope orientation with respect to the north line) is also a common and crucial factor considered to influence the landslide occurrence,

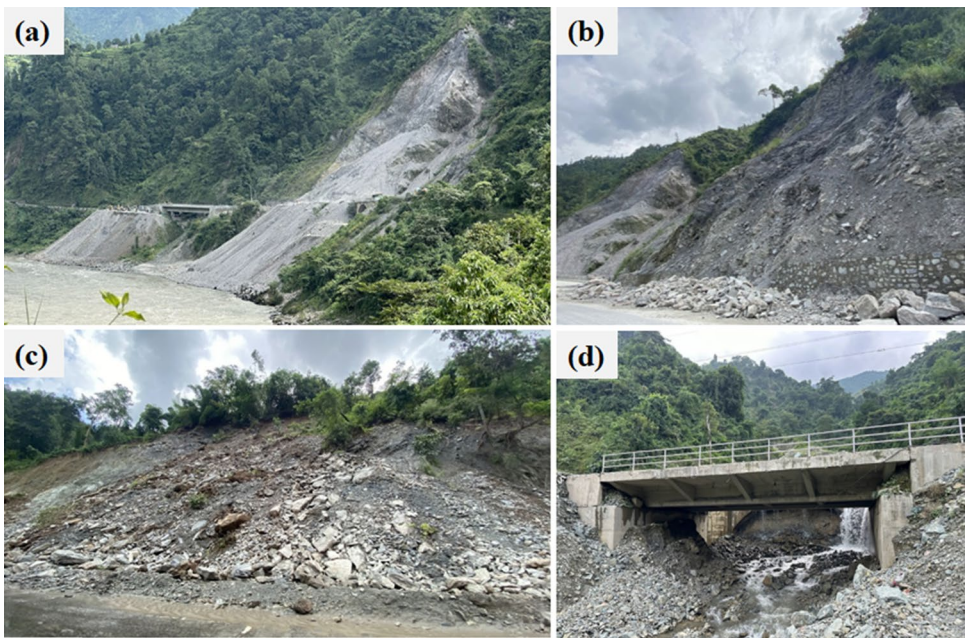

Fig. 3 Field visit photographs: (**a**) landslide near Chandi Bhanjyang (27° 49′ 56.1″ N, 84° 32′ 29.9E) (**b**) landslide at Kalikhola (27° 49′ 13.6″ N, 84° 28′ 56.9″ E) (**c**) landslide near Kabilas (27° 49′ 13.6″ N, 84° 28′ 56.9″ E) (**d**) debris flow impact in Mauri Khola Bridge (27° 49′ 05.0″ N, 84° 27′ 46.7″ E)

as also highlighted by Ercanoglu and Gokceoglu [12], Pourghasemi et al. [25], etc. It essentially indicates the orientation of a terrain surface and influences the amount of solar exposure, drying wind, rainfall, and water flow dynamics within the slope. We derived the slope aspect distribution map from the 30-m DEM data and divided it into the standard nine classes: (i) flat, (ii) north, (iii) northeast, (iv) east, (v) southeast, (vi) south, (vii) southwest, (viii) west, and (ix) northwest.

Profile Curvature The smaller the radius of a curvy ground surface, the greater the curvature, and vice versa. A positive curvature value represents a convex ground surface (i.e., a ridge in cross section), a negative value represents a concave ground surface (i.e., a valley in cross section), and a value of zero (i.e., the curve radius infinitely large) represents a flat terrain. In case of rain as the triggering factor, a concave slope is more likely to fail than a convex slope because the former slope shape has greater tendency to build up subsurface water pressure [15]. In this study, we extracted profile curvature values from the 30-m DEM data and divided them into three classes: (i) concave, (ii) flat, and (iii) convex.

Land Use Land Cover (LULC) Human activities in urbanization, agriculture, and construction work often help alter landscape and LULC affecting the slope soil stability [22]. So, in this study, we used land cover map of Nepal for year 2019 to prepare an LULC map for the analysis and reclassified it into seven categories: (i) water bodies, (ii) forest, (iii) riverbeds, (iv) built-up areas, (v) cropland, (vi) grassland, and (vii) wooded land.

Normalized Difference Vegetative Index (NDVI) NDVI is a measure of green vegetation and biomass density on earth surface, and it plays a crucial role in landslide susceptibility [15]. In general, a negative NDVI value refers to water, 0–0.1 refers to bare riverbeds or sandy areas and a value greater than 0.2 refers to dense vegetation cover. In this study, we used NDVI values of five classes: for Narayanghat–Mugling road section: (i) <0, (ii) 0–0.1, (iii) 0.1–0.15, (iv) 0.15–0.2, and (v) 0.2–0.374,for Mugling-Naubise road section: (i)$-$ 0.16–0.02, (ii) 0.03–0.15, (iii) 0.16–0.25, (iv) 0.26–0.34, and (v) 0.35–0.52; and for Naubise–Kathmandu road section: (i) 0–0.12, (ii) 0.13–0.2, (iii) 0.21–0.27, (iv) 0.28–0.36, and (v) 0.37–0.52.

Proximity to Roads Proximity to roads can significantly affect landslide occurrence by altering landscape and slope soil stability [14, 39]. During the road construction, slope cutting activities significantly alter the natural slope stability. In this work, we applied Euclidean distance method [18] to generate five classes of proximity to roads: (i) 0 to 200 m, (ii) 200–400 m, (iii) 400–600 m, (iv) 600–800 m, and (v) above 800 m.

Proximity to Streams The level of moisture saturation in slope material is a crucial factor in determining the slope stability [44, 45]. Saturated slope soil near the streamside area is highly prone to failure [9, 21]. In this work, we applied Euclidean distance method [18] to generate five classes in this category: (i) 0–200 m, (ii) 200–400 m, (iii) 400–600 m, (iv) 600–800 m, and (v) above 800 m.

Geology The geology of a mountainous or hilly area is an important landslide causal factor that contributes to slope stability or instability of the area. The geological setting characterized by rock types and existence of joints, fractures, faults strongly impact the landslide occurrence in an area [29]. In this work, we referred to a geological map of the study area, published by the Department of Mines and Geology of Nepal in 1994 and reclassified the geology of the area into five groups: (i) Siwalik formation, (ii) Midland formation, (iii) Recent formation, (iv) Pre-Cambrian formation, and (v) Himal formation.

Proximity to Faults The presence of tectonic faults in an area is truly associated with the spatial distribution of landslides and slope failures. In general, landslides are concentrated near the faults, but the landslide density reduces sharply with increasing distance from the faults [30]. Closer fault proximity increases the landslide susceptibility due to relatively high seismicity at the fault planes [15]. The fault proximity buffer zones were divided into the Euclidean distances of 250 m, 500 m, 750 m, 1000 m, and greater than 1000 m.

Annual Rainfall Rainfall (or precipitation) is one of the main triggering factors of landslides and slope failures. Both the rain intensity (mm/h) and amount of rainfall (mm) are considered important in causing landslides. For example, heavy and prolonged rainfall helps increase subsurface water pressure in concave slopes leading to landslide trigger. Rainfall also serves as a climatic factor and contributes to accelerated weathering of rocks. We extracted the annual rainfall data for this study area from the Climate Research Unit's (CRU) database from 2011 to 2020, and reclassified the continuous precipitation values into five equal-interval ranges: for Narayanghat–Mugling road section, (i) 2400–2405 mm, (ii) 2405–2410 mm, (iii) 2410–2415 mm, (iv) 2415–2420 mm, and (v) 2420–2425 mm; for Mugling–Naubise road section, (i) 2083.4–2150, (ii) 2150–2230 mm, (iii) 2230–2310 mm, (iv) 2310–2370 mm, and (v) 2370–2425.4 mm; and for Naubise–Kathmandu road section, (i) 2083.2–2090 mm, (ii) 2090–2095 mm, (iii) 2095–2100 mm, (iv) 2100–2105 mm, and (v) 2105–2109.2 mm.

Method

The accuracy of landslide susceptibility analysis relies upon the selection of appropriate landslide conditioning factors and the quality of landslide inventories. In this study, we picked the above-mentioned 11 landslide conditioning factors on the basis of expert knowledge, extensive field surveys, and literature review. We used ArcGIS 10.8 platform for creating the thematic maps of each landslide conditioning factor in a resolution of 30 m. Since the contribution level of each conditioning factor varies, it is crucial to assess the relative weight of each factor in landslide occurrence [10]. So, the AHP, a multi-criteria method designed for hierarchical decision-making problems was employed for pairwise comparison between all potential pairs of factors contributing to landsliding [34, 36]. The outcome of these comparisons was used to generate a pairwise comparison matrix, where each entry indicates the relative significance of one factor compared to the other. The relative importance between two factors is assessed using a numerical scale, as explained in Table 2. After constructing the matrix, the relative weights of the landslide instability factors were determined through mathematical processing using the AHP algorithm.

Figure 4 outlines the methodological flow of the AHP method-based landslide susceptibility analysis. This method calculates the maximum or principal eigenvector

Table 2 Scale of preference between two parameters in AHP [34]

Preference of factor	Degree of preference	Explanation
1	Equally	Two factors contribute equally to the objective
3	Moderately	Experience and judgment slightly to moderately favor one factor over another
5	Strongly	Experience and judgment strongly or essentially favor over another
7	Very Strongly	A factor is strongly favored over another, and its dominance is shown in practice
9	Extremely	The evidence of favoring one factor over another is the highest degree possible of an affirmation
2,4,6,8	Intermediate	Intermediate use to represent compromises between the preferences in weights 1, 3, 5, 7, and 9
Reciprocals	Opposites	Used for inverse comparison

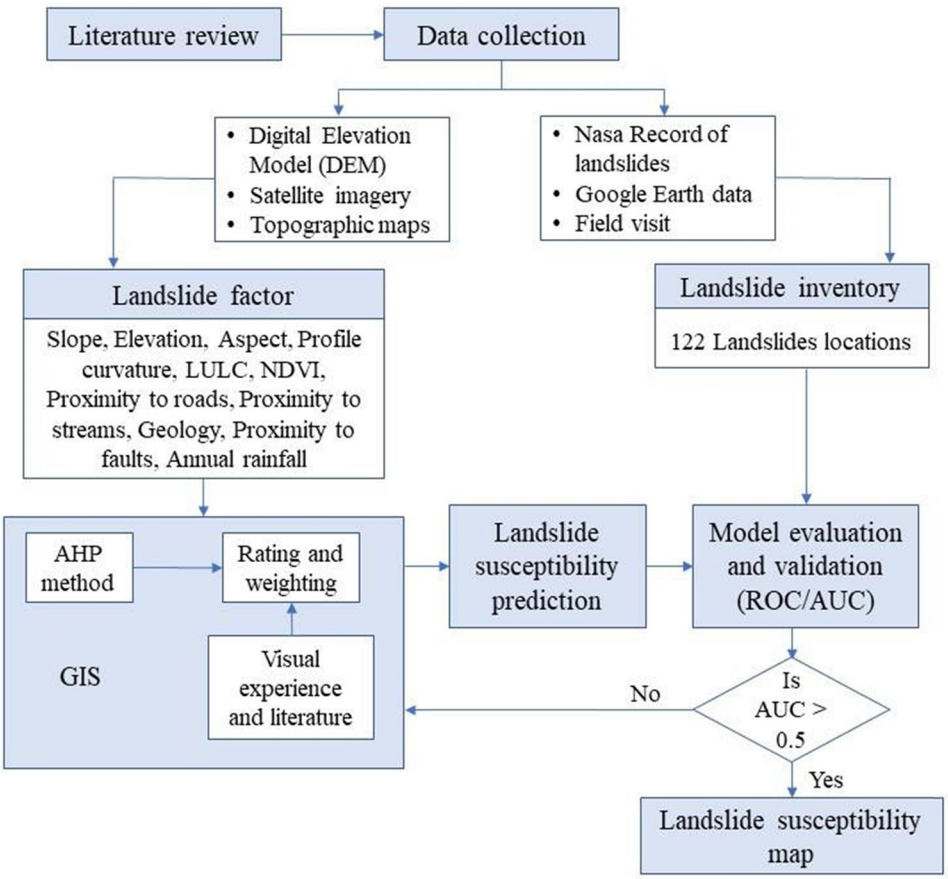

Fig. 4 A methodological flowchart of the landslide susceptibility analysis using AHP

of the matrix. The sum of the eigenvalue equals unity [33]. In the AHP method, the pairwise comparisons in the matrix are considered to be adequately consistent if the corresponding consistency ratio (CR) is less than 0.1 [35], which is calculated using Eq. 1.

$$\mathrm{CR} = \mathrm{CI}/\mathrm{RI} \tag{1}$$

where RI is the random index (refer to Table 3), the value of which depends on the order of the matrix and CI is Consistency Index which is given as:

$$\mathrm{CI} = \left(\lambda_{\max} - \mathrm{n}\right)/(\mathrm{n}-1) \tag{2}$$

where $\lambda_{\max}$ is the largest eigenvalue of the matrix of order n.

Then, the landslide susceptibility index was computed by employing the weighted linear combination equation as:

$$LSI = \sum_{i=1}^{n} R_i W_i \tag{3}$$

where *LSI* is the landslide susceptibility index, *n* is the total number of factors, *Ri* is the rating of the factor *i*, and *Wi* is the weight of the factor *i* (refer to Table 3).

Finally, the computed LSIs were visualized in the form of the landslide susceptibility map in ArcGIS platform, and the roadside landslide hazard characteristics were interpreted using the generated susceptibility map.

Validation

The reliability of the generated landslide susceptibility map was assessed by using area under the receiver operating curve (AUC-ROC) technique. ROC is a commonly used graphical representation that indicates the relationship between true positive and false positive. True positive represents cases where the model correctly predicts the occurrence of a landslide in areas that do experience landslides whereas false positive refers to cases where the model mistakenly identifies a non-landslide prone area as a landslide prone area. The area under the curve (AUC) ranges from 0.5 to 1, and a value greater than 0.5 indicates the model validity and acceptability. The AUC provides a measure of the model accuracy and determines its predictive power. The AUC-ROC in this work was generated by the ArcSDM toolbox in ArcGIS, and later re-plotted in python for better resolution.

Road Infrastructure Vulnerability Assessment

Vulnerability assessment was conducted specifically for the critical infrastructure along the Narayanghat–Kathmandu roadway section integrating both spatial and structural data.

Identification of Elements at Risk

The Narayanghat–Mugling road segment, where all of the road infrastructure—including pavements, drainage systems, and support structures—was rebuilt and finished five years ago, was the focus of the vulnerability assessment. In the last year, all 18 of the bridges along this route that were first completed 45 years ago have been completely replaced with new bridges. Considering this recent reconstruction, the position of these structures in high-susceptibility zones and their possible exposure to landslides have a greater impact on their vulnerability than aging-related deterioration. Although previous maintenance records were not thoroughly examined in this study, long-term performance evaluations could be incorporated into future studies to improve the vulnerability assessment.

In contrast, the Mugling–Kathmandu roadway section is currently undergoing road widening and reconstruction work. Since many of the road infrastructure elements in this section are still being constructed or are in a transitional state, their final configurations and conditions are not yet fixed. As a result, the vulnerability assessment for this section could not be included in this study at this stage, as these structures will be subject to further modification and development.

In the Narayanghat–Mugling roadway section, the key structural components considered in the analysis are:

- *Bridges* Structural components that are highly exposed due to their location across valleys or rivers, making them vulnerable to both direct landslide impact and debris flow.
- *Culverts* Drainage structures vital for water management but prone to blockage or damage during landslide events.
- *Retaining walls* These structures prevent slope failures but are themselves vulnerable to undermining or collapse under excessive landslide forces.

Each of these road structure elements was mapped using GIS-based road network data. The geographic locations and structural characteristics, such as age, material, and condition, were used to create an infrastructure inventory.

Table 3 Random consistency index (RI) [34, 35]

n	1	2	3	4	5	6	7	8	9	10	11	12	13	14	15
RI	0	0	0.58	0.9	1.12	1.24	1.32	1.41	1.45	1.49	1.51	1.53	1.56	1.57	1.59

Vulnerability Index Calculation

The vulnerability index (V_i) for each road infrastructure element was calculated based on the following three key components:

- *Proximity to high-susceptibility zones* The infrastructure elements were overlaid on the landslide susceptibility map produced in "Landslide Susceptibility Mapping" Section. Infrastructure located in areas with high susceptibility scores was assigned higher vulnerability values.
- *Structural fragility* Field inspections were conducted to evaluate the physical condition and design robustness of each infrastructure element. For example, older bridges with visible signs of wear and inadequate maintenance records were considered more fragile, thus receiving higher vulnerability scores.
- *Functional importance* A weighting system was applied to account for the criticality of each element. Bridges and culverts essential for traffic flow were assigned higher weights than less critical components like side drains.

The vulnerability index (V_i) was computed using the following Eq. 4.

$$V_i = P(D_i) \times W_i \tag{4}$$

where $P(D_i)$ represents the probability of damage based on the element's location in a landslide-susceptible zone, and W_i is the weight reflecting the infrastructure's criticality in the road network.

Classification of Vulnerability

The vulnerability index (V_i) was categorized into four levels:

- *Low* Infrastructure elements unlikely to suffer considerable damage due to landslides
- *Moderate* Infrastructure that could experience partial damage but remain functional
- *High* Elements at serious risk of damage, potentially compromising the functionality
- *Very High* Infrastructure at critical risk of failure, requiring immediate intervention

The vulnerability map was produced by integrating the above vulnerability index categories with the road network, identifying the areas where infrastructure is most likely to be affected by landslides.

Risk Assessment

Risk in this study is defined as the potential for loss or damage resulting from the interaction of landslide hazards and the vulnerability of road infrastructure. To quantify this, a risk assessment was performed by integrating the susceptibility and vulnerability layers.

Landslide Hazard and Vulnerability Integration

The landslide risk for each section of road infrastructure was calculated as the product of the landslide hazard (susceptibility) and infrastructure vulnerability:

$$R_i = H_i \times V_i \tag{5}$$

where

- R_i is the risk for infrastructure element iii,
- H_i is the landslide susceptibility score for the location of the infrastructure element, derived from the landslide susceptibility map,
- V_i is the vulnerability index of the infrastructure element, reflecting its exposure and fragility.

We performed a sensitivity study by altering the susceptibility and vulnerability indices within their reasonable ranges in order to verify the robustness of this integration technique. The overall risk classifications (low, moderate, high, and extremely high) stayed constant despite slight variations in the absolute risk values.

Risk Classification

The calculated risk values were classified into four categories:

- *Very low risk* Infrastructure unlikely to be impacted by landslides.
- *Low risk* Infrastructure with minimal risk of damage but may require routine monitoring.
- *Moderate risk* Elements at moderate risk of damage, requiring periodic inspection and maintenance.
- *High risk* Infrastructure at critical risk, demanding immediate intervention and mitigation strategies.

These risk classifications were used to develop a comprehensive landslide risk map for the Narayanghat–Kathmandu road section, highlighting zones that require urgent attention.

Results and Discussion

Landslide Susceptibility Assessment

Figures 5, 6 and 7 are thematic maps of the study area that depict spatial distribution of the 11 landslide conditioning factors (i.e., slope, elevation, aspect, profile curvature, land use and land cover (LULC), normalized difference vegetation index (NDVI), geology, proximity to faults, distance from roads, distance to streams, and annual rainfall) in three road sections of the study area (i.e., Narayanghat–Kathmandu roadway section). A visualization of these maps provides a comprehensive understanding of the terrain characteristics and potential landslide triggers in the region.

The weightage of the factors were provided based on the similar kind of researches and supported by the expert judgment from geotechnical and landslide hazard specialists taking into account field experience. Weight estimates were independently provided by a group of specialists with backgrounds in hazard assessment, remote sensing, and geotechnical engineering. To guarantee the consistency, the weight estimates were then combined using the geometric mean approach. To further investigate the impact of weight fluctuations on the final susceptibility mapping, a sensitivity analysis was performed. The consistency ratio was found to be 0.029, and it is well below the threshold value of 0.1, indicating the validity of pairwise comparison. Figure 8 displays the relative importance of each landslide conditioning factor. As seen in the figure, slope has the highest impact on landslide occurrence with a weightage value of 0.25 in AHP matrix and annual rainfall was found to be the second dominating factor with a weightage value of 0.14 while elevation was found to have the least impact with the lowest weightage of 0.03. Nearly identical to these results, Psomiadis et al. [26] and Leonardi et al. [16] also found slope to be the most significant factor in landslide susceptibility.

The landslide susceptibility map of the study area, categorized into four susceptibility levels using Jenks natural break method is presented in Fig. 9. The natural break susceptibility classes reveal that 6% of the study area has low susceptibility, 42% has moderate susceptibility, 40% has high susceptibility, and 12% has very high susceptibility to landslides. Spatial distribution of the landslide susceptibility indicates that the road section in the western part is far more susceptible to landslides than the eastern one. This is because of steeper slope (i.e., 31°–45°) distribution in the western part than in the eastern part of the road. Moreover, the western part has higher annual rainfall and closer proximity to active faults than the eastern part. The landslide susceptibility analysis provides critical insights in the study area for immediate attention to enhancing mountain road resilience. The high and very high susceptibility zones as identified in all three road segments are highly likely to experience landslides, necessitating immediate mitigation strategies.

Validation of the Landslide Susceptibility Assessment

Figure 10 shows a receiver operating characteristics (ROC) curve obtained for the landslide susceptibility map of Fig. 9, by overlaying the 74 historical landslide locations on the susceptibility map. From the area under the ROC curve, the prediction rate was found to be 75.1%, which validates the landslide susceptibility map of Fig. 9. Although the susceptibility assessment's validity is supported by this AUC result, it is important to recognize several possible sources of error and accuracy limitations. First, as some historical landslides might not have been precisely documented or mapped, the completeness and quality of the landslide inventory dataset may have an impact on model performance. Second, spatial errors may be introduced by the resolution of the input data, such as the 30-m DEM utilized for terrain-related metrics. Third, even with expert judgement and sensitivity analysis, the final susceptibility scores may be impacted by the subjectivity of AHP weight assignment. Lastly, the model's capacity to accurately depict landslide-prone regions may be constrained by the omission of other contributing elements, such as soil characteristics in different depths and seismic activity.

Vulnerability Assessment

The vulnerability assessment of bridges, culverts, and retaining walls along the Narayanghat–Mugling road section identified significant spatial variability in infrastructure vulnerability to landslide events (Fig. 11). The analysis focused on the proximity of infrastructure to high-susceptibility zones, structural fragility, and functional importance. Each category of infrastructure exhibited varying degrees of vulnerability based on its location and condition.

For the bridges, 18 structures were analyzed with results indicating that eight bridges (equivalent to 44.44%) are in very high vulnerability zones, mainly due to their location near steep slopes, rivers, and fault lines, which raise the risk of structural damage by landslides. Five bridges were assessed to be in high vulnerability class, four bridges in moderate vulnerability, and one in low vulnerability class. This variation reflects differences in location, design, and condition, where newer or better-maintained bridges were assessed to be in lower vulnerability class.

Culverts were also assessed for the vulnerability. Out of the 77 culverts assessed, 25 were found to be in very high vulnerability zones and 28 in high vulnerability zones, indicating a high likelihood of blockage or overflow during landslide events. The assessment also revealed that 18 culverts are in moderate vulnerability class and six in low

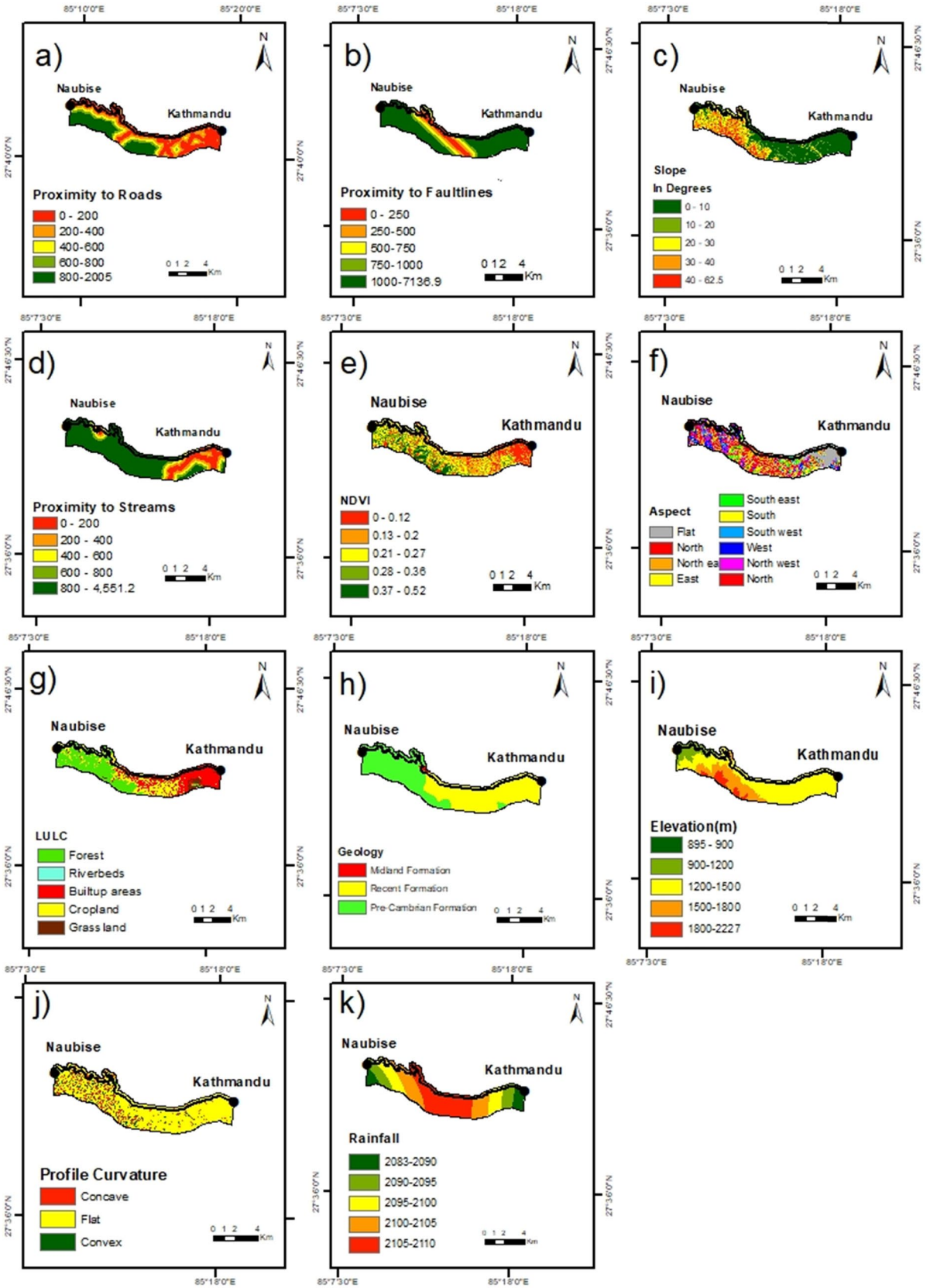

Fig. 5 Thematic maps of the landslide conditioning factors of Narayanghat–Mugling road section: (**a**) proximity to roads, (**b**) proximity to fault lines, (**c**) slope, (**d**) proximity to streams, (**e**) NDVI, (**f**) aspect, (**g**) LULC, (**h**) geology, (**i**) elevation, (**j**) profile curvature, and (**k**) rainfall

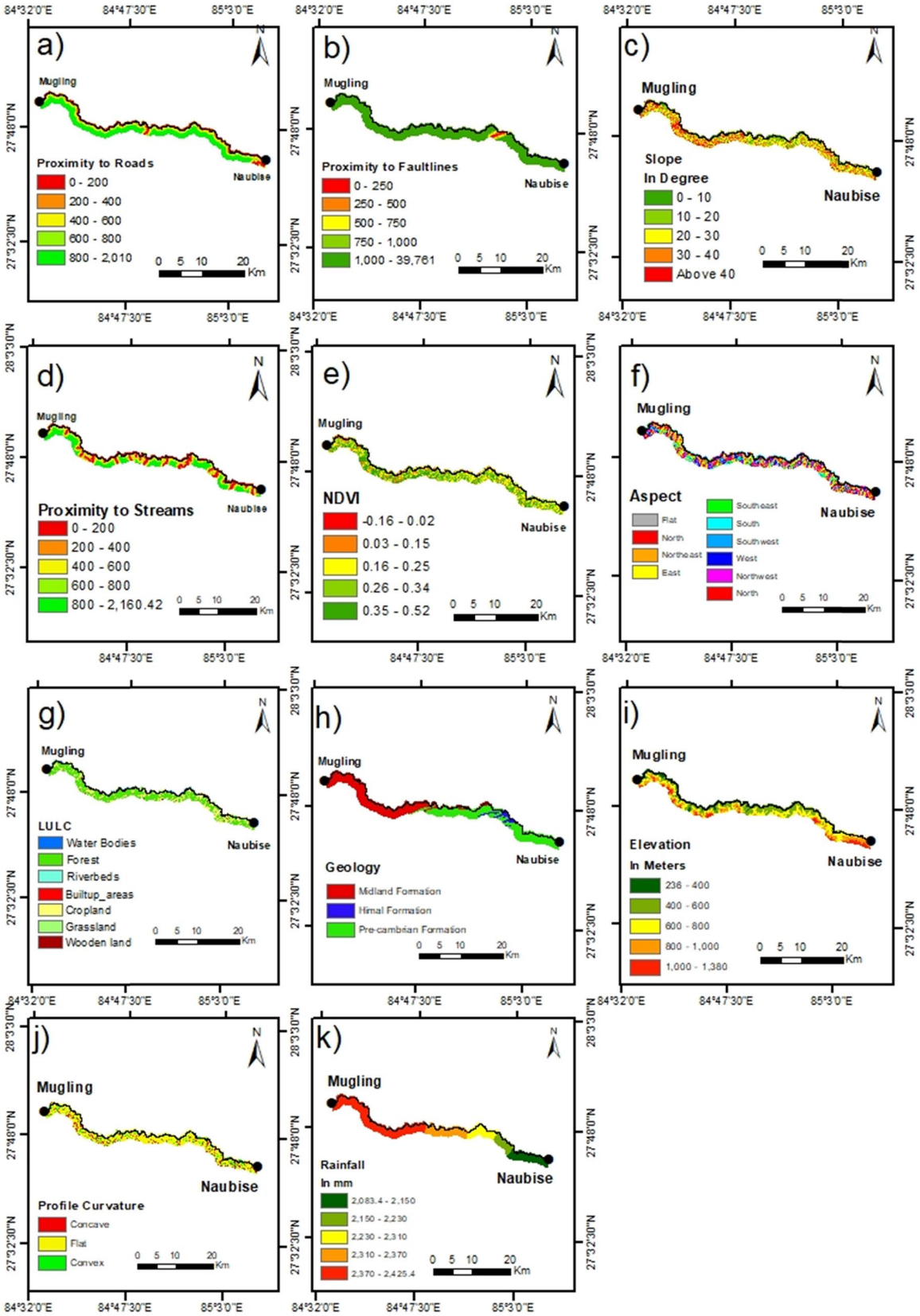

Fig. 6 Thematic maps of the landslide conditioning factors of Mugling–Naubise road section: (**a**) proximity to roads, (**b**) proximity to fault lines, (**c**) slope, (**d**) proximity to streams, (**e**) NDVI, (**f**) aspect, (**g**) LULC, (**h**) geology, (**i**) elevation, (**j**) profile curvature, and (**k**) rainfall

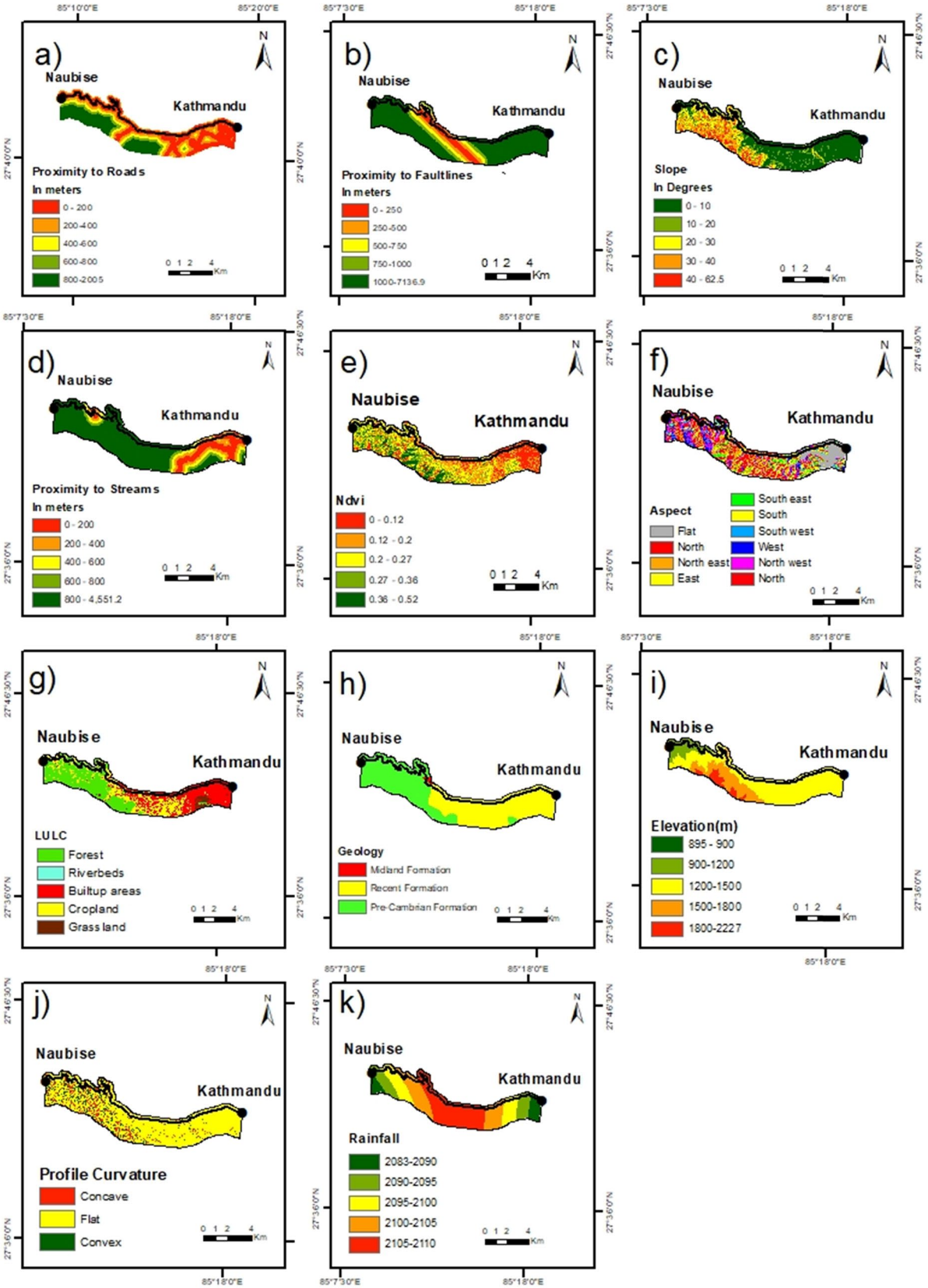

Fig. 7 Thematic maps of the landslide conditioning factors of Naubise–Kathmandu road section: (**a**) proximity to roads, (**b**) proximity to fault lines, (**c**) slope, (**d**) proximity to streams, (**e**) NDVI, (**f**) aspect, (**g**) LULC, (**h**) geology, (**i**) elevation, (**j**) profile curvature, and (**k**) rainfall

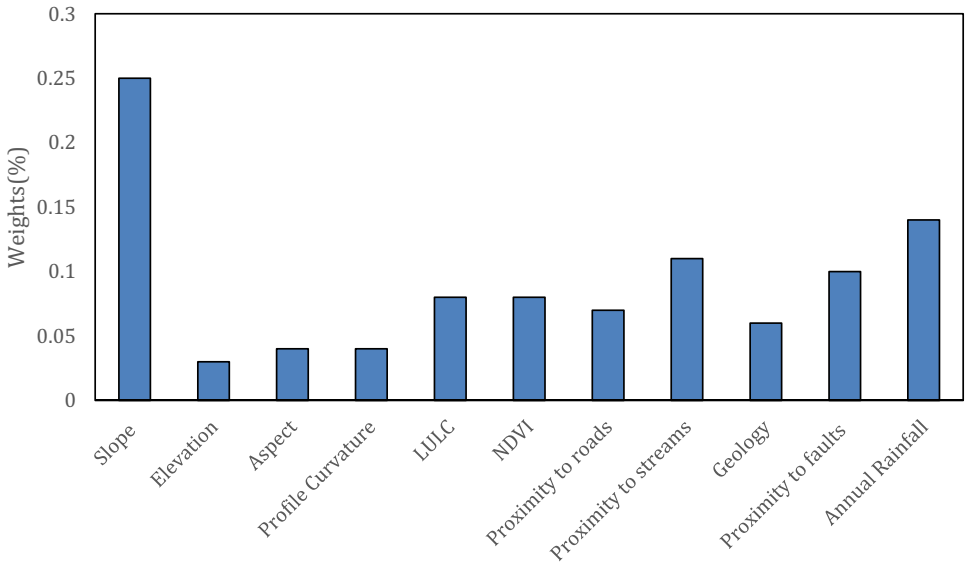

Fig. 8 Results of pairwise comparisons of the landslide conditioning factors for the landslide susceptibility assessment

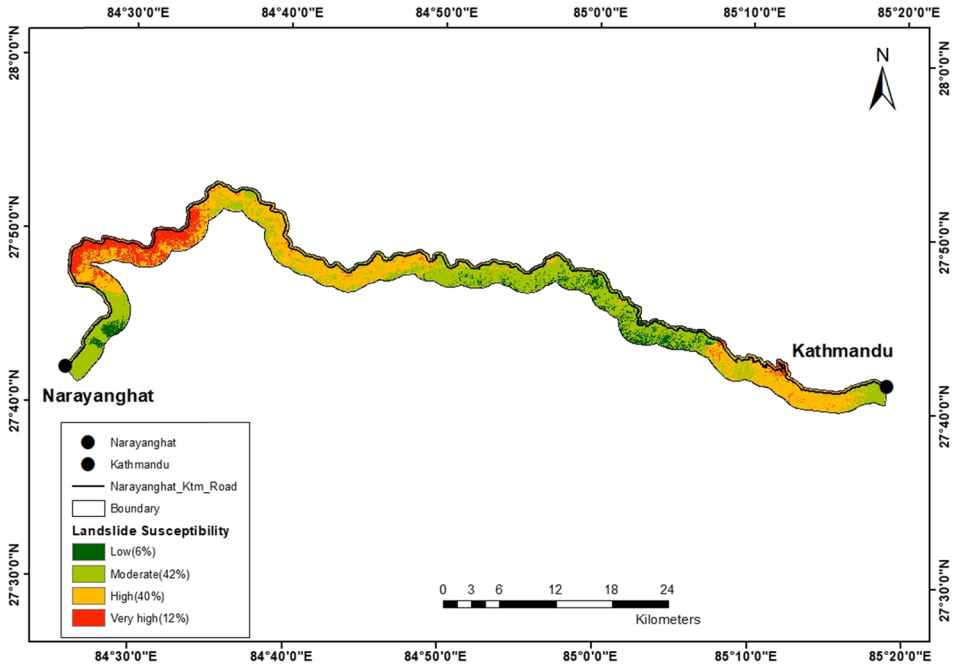

Fig. 9 Landslide susceptibility map of the study area (i.e., Narayanghat–Kathmandu road section)

vulnerability class. These culverts are primarily away from steep slopes or active landslide areas and have robust structural design.

In case of retaining walls, 23 out of the 52 assessed structures were assessed to be in very high vulnerability class, posing a significant risk of failure under heavy landslide pressures. Another 22 retaining walls were assessed to be highly vulnerable, suggesting that they are also at risk but less likely to fail compared to those in the very high vulnerability class. The remaining seven retaining walls were found to be moderately vulnerable while none of them were assessed to be in low vulnerability class, which indicates that the area is susceptible to landslides alone and there is a need of robust landslide stabilization measures.

Landslide Risk Assessment

Figure 12 shows the results of road section risk assessment conducted by integrating the landslide susceptibility and road infrastructure (i.e., bridges, culverts, and retaining walls). Of the 18 bridges assessed, five are found to be at very high risk, probably due to their proximity to steep slopes, rivers, and fault lines, coupled with high vulnerability scores indicating structural fragility and critical

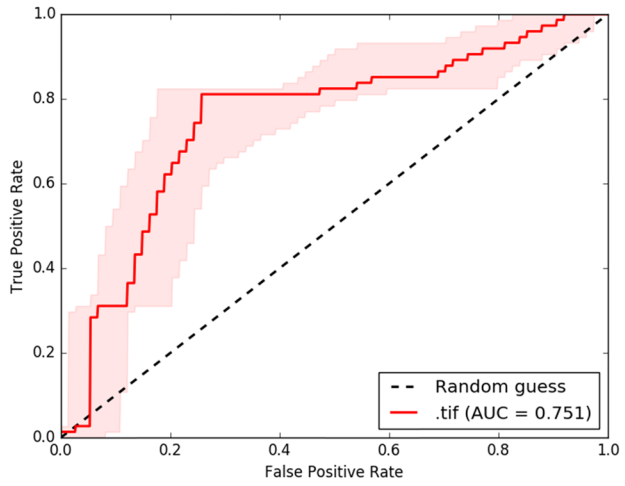

Fig. 10 ROC for susceptibility simulation (prediction rate)

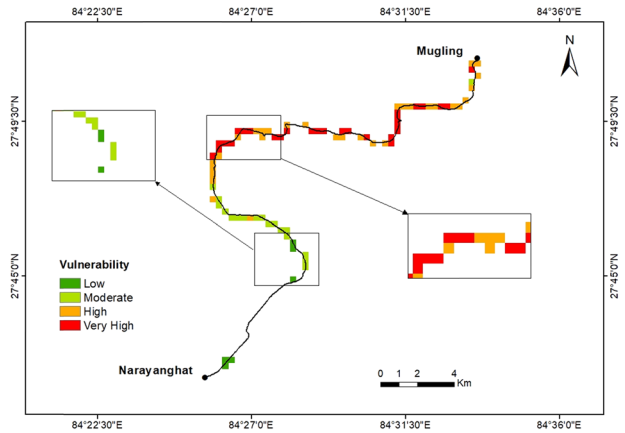

Fig. 11 Road infrastructure vulnerability assessment in the Narayanghat–Mugling road section

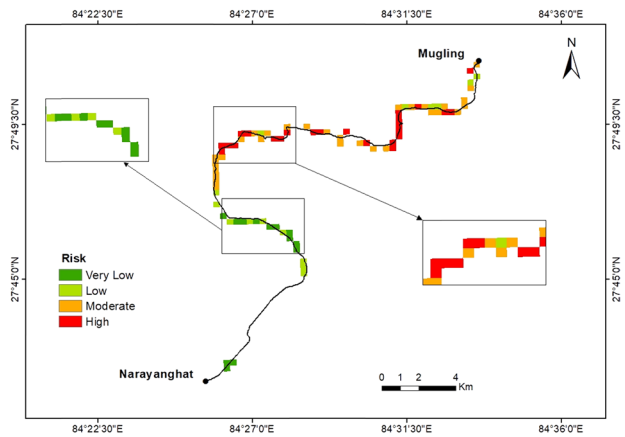

Fig. 12 Landslide risk map of the Narayanghat–Mugling road section

importance. Four bridges are at high risk, with moderate landslide susceptibility but high vulnerability due to structural age or maintenance issues. The rest are at moderate and low risk, reflecting safer locations or robust conditions.

Of the 77 culverts assessed, 21 were identified as being at very high risk, mainly due to their high likelihood of blockage in landslide-prone areas. Another 18 are at high risk, while 9 and 8 are at moderate and low risk, respectively, reflecting safer locations or effective drainage designs.

Retaining walls also at significant risk, with 15 out of 42 categorized as being at very high risk due to their exposure to high susceptibility zones and structural concerns. 14 are at high risk, while 10 and 3 are at moderate and low risk, respectively, indicating effective stabilization measures in these areas.

The integration of vulnerability into risk assessment provides a nuanced understanding of why certain structures are at higher risk. For example, even if a bridge is located in a moderate susceptibility zone, high vulnerability (such as due to structural fragility or critical importance) can elevate the risk level. Conversely, robust, well-maintained infrastructure in high susceptibility zones may still score lower on the risk scale. This combined approach enables more precise targeting of mitigation strategies, highlighting where slope stabilization, drainage improvements, or structural reinforcements are most urgently needed.

Conclusion

The risk of roadside landslides and slope failures and their impact on critical road infrastructure in the Narayanghat–Kathmandu road section of Nepal were assessed in this study. By evaluating both the landslide susceptibility and the vulnerability of road infrastructure, we conducted a comprehensive landslide risk analysis for a 146-km landslide-prone primary road section of Nepal. Our findings reveal that 12% of the study area lies in very high landslide susceptibility class, 40% lies in high landslide susceptibility class, 42% lies in moderate landslide susceptibility class, and only 6% lies in low landslide susceptibility class. Likewise, the vulnerability assessment results indicate varying levels of infrastructure vulnerability along a 36-km road section from Narayanghat to Mugling.

The risk analysis, a result of landslide susceptibility and infrastructure vulnerability integration, revealed that the northern part of the Narayanghat–Mugling road section of the road is more exposed to landslide risk than the southern section. Specific infrastructure, including 5 bridges, 21 culverts, and 15 retaining walls were assessed to be situated in very high-risk zones. These findings emphasize the exposure of the road network to landslide hazards and underscore the

importance of targeted interventions to enhance the resilience of road infrastructure.

This study provides valuable insights for the policymakers and transportation planners to mitigate the landslide impacts on roadway infrastructure, improve safety, and enhance the reliability of transportation routes in mountainous areas. The results can inform the prioritization of mitigation measures, such as slope stabilization, drainage improvements, and infrastructure reinforcement to reduce the risk posed by landslides to critical road infrastructure.

However, one notable limitation of this study is exclusion of debris flows potentially originating from locations far from the roadway, which may also affect the road infrastructure elements like bridges. Future research is intended to incorporate such hazards so as to provide a more comprehensive understanding of the risk in mountain road networks. Expanding the scope to include additional geohazards will contribute to a more holistic risk assessment and better-informed strategies for protecting the transportation infrastructure in landslide-prone areas.

Acknowledgements The authors would like to appreciate the help received from the Department of Roads in availing the valuable data required for this research work. Special thanks are also extended to Indra Prasad Acharya (an Associate Professor of the Institute of Engineering, Pulchowk Campus, Tribhuvan University) for providing the first author some valuable suggestions while conceptualizing this research work.

Funding For this study, the authors received no funding from any external sources.

Data availability The data used in this study will be availed upon a reasonable request.

Declarations

Conflict of interest The authors declare that they have no conflicts of interest in relation to the work done in this study and in publishing this paper.

References

1. Adhikari BR, Tian B (2021) Spatiotemporal distribution of landslides in Nepal. In Handbook of disaster risk reduction for resilience, Springer, pp 453–471
2. Ahmed B (2015) Landslide susceptibility modelling applying user-defined weighting and data-driven statistical techniques in Cox's Bazar Municipality, Bangladesh. Nat Hazards 79(3):1707–1737
3. Ali S, Biermanns P, Haider R, Reicherter K (2019) Landslide susceptibility mapping by using a geographic information system (GIS) along the China-Pakistan economic corridor (Karakoram Highway), Pakistan. Nat Hazard 19(5):999–1022
4. Alsabhan AH, Singh K, Sharma A, Alam S, Pandey DD, Rahman SAS, Khursheed A, Munshi FM (2022) Landslide susceptibility assessment in the Himalayan range based along Kasauli–Parwanoo road corridor using weight of evidence, information value, and frequency ratio. J King Saud Univ-Sci 34(2):101759
5. Arrogante-Funes P, Bruzón AG, Arrogante-Funes F, Ramos-Bernal RN, Vázquez-Jiménez R (2021) Integration of vulnerability and hazard factors for landslide risk assessment. Int J Environ Res Public Health 18(22):11987
6. Beigh IH, Bukhari SK (2024) Comparative analysis of GIS-based quantitative approaches for landslide susceptibility assessment along national highway-1(NH-1), north Kashmir Himalaya, India. Indian Geotech J. https://doi.org/10.1007/s40098-024-01012-6
7. Bhandary NP, Yatabe R, Hasegawa S, Dahal RK (2011) Characteristic features of deep-seated landslides in Mid-Nepal Himalayas: spatial distribution and mineralogical evaluation. In: Geo-frontiers 2011: advances in geotechnical engineering, pp 1693–1702
8. Chuvieco E, Martínez S, Román MV, Hantson S, Pettinari ML (2014) Integration of ecological and socio-economic factors to assess global vulnerability to wildfire. Glob Ecol Biogeogr 23(2):245–258
9. Dai FC, Lee CF, Ngai YY (2002) Landslide risk assessment and management: an overview. Eng Geol 64(1):65–87
10. Dhungana G, Ghimire R, Poudel R, Kumal S (2023) Landslide susceptibility and risk analysis in Benighat rural municipality, Dhading. Nepal Nat Hazards Res 3(2):170–185
11. DWIDP (2003) Disaster review 2003. An annual publication of the department of water induced disaster prevention, Nepal
12. Ercanoglu M, Gokceoglu C (2004) Use of fuzzy relations to produce landslide susceptibility map of a landslide prone area (West Black Sea Region, Turkey). Eng Geol 75(3–4):229–250
13. Jhinkwan VS, Chore HS, Kumar A (2024) Assessment of stability of slopes and remedial measures in Lesser Himalayan Region: an overview. Indian Geotech J. https://doi.org/10.1007/s40098-024-01047-9
14. Kavzoglu T, Colkesen I (2009) A kernel functions analysis for support vector machines for land cover classification. Int J Appl Earth Obs Geoinf 11(5):352–359
15. Khatakho R, Gautam D, Aryal KR, Pandey VP, Rupakhety R, Lamichhane S, Liu Y-C, Abdouli K, Talchabhadel R, Thapa BR (2021) Multi-hazard risk assessment of Kathmandu Valley. Nepal Sustainab 13(10):5369
16. Leonardi G, Palamara R, Manti F, Tufano A (2022) GIS-multicriteria analysis using AHP to evaluate the landslide risk in road lifelines. Appl Sci 12(9):4707
17. Liu Q, Tang A, Huang D, Huang Z, Zhang B, Xu X (2022) Total probabilistic measure for the potential risk of regional roads exposed to landslides. Reliab Eng Syst Saf 228:108822
18. Longley PA, Goodchild MF, Maguire DJ, Rhind DW (2015) Geographic information systems and science, 4th edn. Wiley
19. Lu Q-C, Xu P-C, Zhang J (2021) Infrastructure-based transportation network vulnerability modeling and analysis. Physica A 584:126350
20. Mosaffaie J, Salehpour Jam A, Sarfaraz F (2024) Landslide risk assessment based on susceptibility and vulnerability. Environ Dev Sustain 26(4):9285–9303. https://doi.org/10.1007/s10668-023-03093-4
21. Ntelis G, Maria S, Efthymios L (2019) Landslide susceptibility estimation using GIS. Evritania prefecture: a case study in Greece. J Geosci Enviro Protect 7(8):206–220
22. Pacheco Quevedo R, Velastegui-Montoya A, Montalván-Burbano N, Morante-Carballo F, Korup O, Daleles Rennó C (2023) Land use and land cover as a conditioning factor in landslide susceptibility: a literature review. Landslides 20(5):967–982
23. Panchal S, Shrivastava AK (2022) Landslide hazard assessment using analytic hierarchy process (AHP): a case study of National Highway 5 in India. Ain Shams Eng J 13(3):101626

24. Pantha BR, Yatabe R, Bhandary NP (2010) GIS-based highway maintenance prioritization model: an integrated approach for highway maintenance in Nepal mountains. J Transp Geogr 18(3):426–433
25. Pourghasemi HR, Pradhan B, Gokceoglu C, Mohammadi M, Moradi HR (2013) Application of weights-of-evidence and certainty factor models and their comparison in landslide susceptibility mapping at Haraz watershed. Iran Arab J Geosci 6:2351–2365
26. Psomiadis E, Papazachariou A, Soulis KX, Alexiou D-S, Charalampopoulos I (2020) Landslide mapping and susceptibility assessment using geospatial analysis and earth observation data. Land 9(5):133
27. Qadami BS, Oujidi M, Ejjaouani H et al (2023) A study of network roads landslides and their stabilization methods in Fahs Anjra Province: north of Morocco. Indian Geotech J 53:593–612. https://doi.org/10.1007/s40098-022-00696-y
28. Rahman G, Bacha AS, Ul Moazzam MF, Rahman AU, Mahmood S, Almohamad H, Al Dughairi AA, Al-Mutiry M, Alrasheedi M, Abdo HG (2022) Assessment of landslide susceptibility, exposure, vulnerability, and risk in shahpur valley, eastern hindu kush. Front Earth Sci 10:953627
29. Rahmati O, Yousefi S, Kalantari Z, Uuemaa E, Teimurian T, Keesstra S, Pham TD, Tien Bui D (2019) Multi-hazard exposure mapping using machine learning techniques: a case study from Iran. Remote Sens 11(16):1943
30. Regmi AD, Devkota KC, Yoshida K, Pradhan B, Pourghasemi HR, Kumamoto T, Akgun A (2014) Application of frequency ratio, statistical index, and weights-of-evidence models and their comparison in landslide susceptibility mapping in Central Nepal Himalaya. Arab J Geosci 7:725–742
31. Regmi AD, Yoshida K, Nagata H, Pradhan AMS, Pradhan B, Pourghasemi HR (2013) The relationship between geology and rock weathering on the rock instability along Muglin–Narayanghat road corridor, Central Nepal Himalaya. Nat Hazards 66:501–532
32. Rehman S, Azhoni A (2023) Analyzing landslide susceptibility, health vulnerability and risk using multi-criteria decision-making analysis in Arunachal Pradesh. India Acta Geophys 71(1):101–128
33. Reis S, Yalcin A, Atasoy M, Nisanci R, Bayrak T, Erduran M, Sancar C, Ekercin S (2012) Remote sensing and GIS-based landslide susceptibility mapping using frequency ratio and analytical hierarchy methods in Rize province (NE Turkey). Environ Earth Sci 66:2063–2073
34. Saaty TL (1977) A scaling method for priorities in hierarchical structures. J Math Psychol 15(3):234–281
35. Saaty TL (1980) The analytic hierarchy process: planning, priority setting, resource allocation. McGraw-Hill, New York
36. Saaty TL (2006) Rank from comparisons and from ratings in the analytic hierarchy/network processes. Eur J Oper Res 168(2):557–570
37. Singh A, Pal S, Kanungo DP (2021) An integrated approach for landslide susceptibility–vulnerability–risk assessment of building infrastructures in hilly regions of India. Environ Dev Sustain 23(4):5058–5095
38. Singh K, Kumar V (2018) Hazard assessment of landslide disaster using information value method and analytical hierarchy process in highly tectonic Chamba region in bosom of Himalaya. J Mt Sci 15(4):808–824
39. Skilodimou HD, Bathrellos GD, Chousianitis K, Youssef AM, Pradhan B (2019) Multi-hazard assessment modeling via multi-criteria analysis and GIS: a case study. Environ Earth Sci 78:1–21
40. Subedi L, Acharya KK (2016) Tracing the Mahabharat Thrust (MT) on the basis of lithology and microstructures around Bhainse–Manahari area, central Nepal. J Nepal Geol Soc 51:39–48
41. Sur U, Singh P, Meena SR (2020) Landslide susceptibility assessment in a lesser Himalayan road corridor (India) applying fuzzy AHP technique and earth-observation data. Geomatics Nat Hazards Risk 11(1):2176–2209. https://doi.org/10.1080/19475705.2020.1836038
42. Tesfa C (2024) Geohazard mapping and mitigations of landslides along the road corridor Gasera-Indeto, Oromia Regional State, Southeast Ethiopia. Indian Geotech J. https://doi.org/10.1007/s40098-024-01084-4
43. Timilsina M, Dahal RK (2013) Landslide hazard in Muglin Road. Int J Landslide Environ 1(1):105–106
44. Yalcin A (2008) GIS-based landslide susceptibility mapping using analytical hierarchy process and bivariate statistics in Ardesen (Turkey): comparisons of results and confirmations. CATENA 72(1):1–12
45. Yalcin A, Bulut F (2007) Landslide susceptibility mapping using GIS and digital photogrammetric techniques: a case study from Ardesen (NE-Turkey). Nat Hazards 41(1):201–226
46. Yoshida K (2013) Landslide susceptibility mapping using certainty factor, index of entropy and logistic regression models in GIS. Nat Hazards 65:135–165
47. Yu H, Pei W, Zhang J, Chen G (2023) Landslide susceptibility mapping and driving mechanisms in a vulnerable region based on multiple machine learning models. Rem Sens 15(7):1886
48. Yu X, Zhang K, Song Y, Jiang W, Zhou J (2021) Study on landslide susceptibility mapping based on rock–soil characteristic factors. Sci Rep 11(1):15476
49. Zhou M, Yuan M, Yang G, Mei G (2023) Risk analysis of road networks under the influence of landslides by considering landslide susceptibility and road vulnerability: a case study. *Nat Hazards Res*
50. Zou Q, Cui P, Zhou GGD, Li S, Tang J, Li S (2018) A new approach to assessing vulnerability of mountain highways subject to debris flows in China. Progress Phys Geogr: Earth Environ 42(3):305–329